

Leptogenesis scenarios for natural SUSY with mixed axion-higgsino dark matter

Kyu Jung Bae^{a,b}, Howard Baer^a, Hasan Serce^a and Yi-Fan Zhang^a

^a*Dept. of Physics and Astronomy, University of Oklahoma, Norman, OK 73019, USA*

^b*Dept. of Physics, University of Tokyo, Bunkyo-ku, Tokyo 113-0033, Japan*

E-mail: bae@hep-th.phys.s.u-tokyo.ac.jp, baer@nhn.ou.edu, serce@ou.edu, zyf@ou.edu

ABSTRACT: Supersymmetric models with radiatively-driven electroweak naturalness require light higgsinos of mass $\sim 100 - 300$ GeV. Naturalness in the QCD sector is invoked via the Peccei-Quinn (PQ) axion leading to mixed axion-higgsino dark matter. The SUSY DFSZ axion model provides a solution to the SUSY μ problem and the Little Hierarchy $\mu \ll m_{3/2}$ may emerge as a consequence of a mismatch between PQ and hidden sector mass scales. The traditional gravitino problem is now augmented by the axino and saxion problems, since these latter particles can also contribute to overproduction of WIMPs or dark radiation, or violation of BBN constraints. We compute regions of the T_R vs. $m_{3/2}$ plane allowed by BBN, dark matter and dark radiation constraints for various PQ scale choices f_a . These regions are compared to the values needed for thermal leptogenesis, non-thermal leptogenesis, oscillating sneutrino leptogenesis and Affleck-Dine leptogenesis. The latter three are allowed in wide regions of parameter space for PQ scale $f_a \sim 10^{10} - 10^{12}$ GeV which is also favored by naturalness: $f_a \sim \sqrt{\mu M_P / \lambda_\mu} \sim 10^{10} - 10^{12}$ GeV. These f_a values correspond to axion masses somewhat above the projected ADMX search regions.

KEYWORDS: axions, dark matter, baryogenesis, leptogenesis, Affleck-Dine, DFSZ, KSVZ, supersymmetry, WIMPs.

1. Introduction

1.1 Electroweak naturalness

The recent discovery of the Higgs boson with mass $m_h \simeq 125$ GeV at LHC8 [1, 2] brings with it a puzzle: why is the Higgs so light when its mass is quadratically divergent? Supersymmetry provides an elegant solution to this so-called naturalness problem by providing order-by-order cancellation of quadratic divergences. In fact, in the Minimal Supersymmetric Standard Model or MSSM, the Higgs mass is constrained so that $m_h \lesssim 135$ GeV [3]: the measured mass lies comfortably below this bound. The price to pay for a SUSY solution to the electroweak naturalness problem is that, naively, superpartners also ought to exist at or around the weak scale m_{weak} as typified by the W , Z and h masses: $m_{\text{weak}} \sim 100$ GeV. However, null results from sparticle searches at LHC8 have resulted in mass limits within the multi-TeV regime [4, 5]: $m_{\tilde{g}} \gtrsim 1.3$ TeV for $m_{\tilde{g}} \ll m_{\tilde{q}}$ and $m_{\tilde{g}} \gtrsim 2$ TeV for $m_{\tilde{q}} \sim m_{\tilde{g}}$. Furthermore, the somewhat large value of m_h seems to require either well-mixed TeV scale top-squarks or 10-100 TeV top-squarks with small mixing [6, 7]. These rather large sparticle mass values threaten to re-introduce the naturalness question: this time due to log divergences which emerge from the Little Hierarchy $m_{\text{weak}} \ll m_{\text{sparticle}} \sim 2 - 20$ TeV. Some authors go so far as to claim the emergent Little Hierarchy leads to a crisis in physics [8]. To proceed at a deeper level, a quantitative discussion of SUSY electroweak naturalness is warranted.

The weak scale as typified by the Z -boson mass is directly related to weak scale SUSY Lagrangian parameters via the well-known scalar potential minimization condition

$$\frac{m_Z^2}{2} = \frac{(m_{H_d}^2 + \Sigma_d^d) - (m_{H_u}^2 + \Sigma_u^u) \tan^2 \beta}{(\tan^2 \beta - 1)} - \mu^2 \quad (1.1)$$

$$\simeq -m_{H_u}^2 - \mu^2 - \Sigma_u^u(i) \quad (1.2)$$

where $m_{H_u}^2$ and $m_{H_d}^2$ are the *weak scale* soft SUSY breaking Higgs masses, μ is the *supersymmetric* higgsino mass term and Σ_u^u and Σ_d^d contain an assortment of loop corrections (labelled by index i) to the effective potential (the complete set of one-loop corrections is given in Ref. [9]). The *electroweak fine-tuning measure* Δ_{EW} [9] compares the largest contribution on the right-hand-side of Eq. 1.2 to the value of $m_Z^2/2$. If they are comparable, then no unnatural fine-tunings are required to generate $m_Z = 91.2$ GeV. The measure Δ_{EW} has the advantage of being model-independent (in that any model yielding the same weak scale spectra will have the same value of Δ_{EW}). It is also pragmatic: in computer codes that calculate the weak scale SUSY spectra, this is the point where actual fine-tuning occurs - usually in the form of dialing the required value of μ so as to ensure that $m_Z = 91.2$ GeV. The implications of natural SUSY (SUSY spectra with low $\Delta_{\text{EW}} \lesssim 30$ [10]) are as follows [9].

- $\mu \sim 100 - 300$ GeV (the lighter the better) leading to a set of light higgsinos $\tilde{Z}_{1,2}$ and \tilde{W}_1^\pm . The \tilde{Z}_1 is the lightest SUSY particle (LSP) and it is a higgsino-like WIMP which is thermally under-produced as a dark matter candidate.

- The soft term $m_{H_u}^2$ is driven radiatively to small values $\sim -(100 - 300)^2 \text{ GeV}^2$ at the weak scale (this is known as radiatively-driven naturalness or RNS). This can always occur in models with high scale Higgs soft term non-universality.
- The radiative corrections Σ_u^u are $\lesssim (100 - 300)^2 \text{ GeV}^2$. The largest of these usually comes from the top squark contributions $\Sigma_u^u(\tilde{t}_{1,2})$. These contributions can both be small for well-mixed (large A_t) top squarks with mass $m_{\tilde{t}_1} \lesssim 4 \text{ TeV}$ and $m_{\tilde{t}_2} \lesssim 10 \text{ TeV}$. These same conditions lift m_h into the 125 GeV vicinity.

While a value of low Δ_{EW} seems like a necessary condition for SUSY naturalness, the question is: is it also sufficient? Does it embody high scale fine-tuning as well? The answer given in Ref's [11, 12] is that, yes, Eq. 1.2 provides a complete portrayal of SUSY electroweak fine-tuning.

- An often-invoked alternative known as Higgs mass fine-tuning requires no large cancellations in contributions to the Higgs boson mass: $m_h^2 \sim \mu^2 + m_{H_u}^2 + \delta m_{H_u}^2$ and thus requires $\delta m_{H_u}^2 \lesssim m_h^2$. The value of $\delta m_{H_u}^2$ can be calculated by integrating the renormalization group equation for the soft term $m_{H_u}^2$. A back-of-the-envelope evaluation leads to $\delta m_{H_u}^2 \sim -\frac{3f_t^2}{8\pi^2}(m_{Q_3}^2 + m_{U_3}^2 + A_t^2) \ln(\Lambda^2/m_{\text{SUSY}}^2)$ where Λ is the high scale usually taken to be m_{GUT} and $m_{\text{SUSY}} \sim 1 \text{ TeV}$. However, this overly simplified expression neglects the fact that $m_{H_u}^2$ itself feeds into the evaluation of $\delta m_{H_u}^2$. In fact, the larger the value of $m_{H_u}^2(\Lambda)$, then the larger is the cancelling correction $\delta m_{H_u}^2$. This evaluation violates the *fine-tuning rule* [12]: to avoid over-estimates of fine-tuning, first combine *dependent* contributions to any observable quantity. By following the fine-tuning rule, then instead the two terms on the RHS of $m_h^2 = \mu^2 + (m_{H_u}^2(\Lambda) + \delta m_{H_u}^2)$ should be comparable to m_h^2 . Since $m_{H_u}^2(\Lambda) + \delta m_{H_u}^2 = m_{H_u}^2(\text{weak})$, then the Higgs mass fine-tuning conditions lead to the same as those for low Δ_{EW} .
- EENZ/BG fine-tuning [13, 14] $\Delta_{\text{BG}} = \max_i \left| \frac{\partial \ln m_Z^2}{\partial \ln p_i} \right|$ measures the sensitivity of m_Z^2 to high scale parameters p_i . The usual application of Δ_{BG} is to multi-parameter effective theories where the various p_i parametrize our ignorance of the nature of the hidden sector which serves as an arena for SUSY breaking. By recognizing that in any SUGRA theory the soft terms are all calculated as multiples of the gravitino mass $m_{3/2}$, then the Z mass can be expressed in terms of high scale parameters as $m_Z^2 \simeq -2\mu^2(\Lambda) + a \cdot m_{3/2}^2$. Since μ hardly evolves, then $a \cdot m_{3/2}^2 \simeq m_{H_u}^2(\text{weak})$ so that a low value of Δ_{BG} leads again to the same requirements as a low value of Δ_{EW} .

1.2 Naturalness in the QCD sector

In QCD, in the limit of two light quarks u, d , one has an approximate global $U(2)_L \times U(2)_R$ chiral symmetry which can be recast as $U(2)_V \times U(2)_A$. The vector symmetry leads to well-known SU(2) of isospin along with baryon number conservation. The axial $U(2)_A$ symmetry is spontaneously broken and naively leads to four instead of three light pions as pseudo-Goldstone bosons. Weinberg suggested [15] the $U(1)_A$ symmetry was somehow not respected and indeed this viewpoint was vindicated by 't Hooft's discovery of the

QCD θ vacuum. A consequence of this resolution of the $U(1)_A$ problem is that the QCD Lagrangian should contain a C and CP -violating term

$$\mathcal{L}_{\text{QCD}} \ni \frac{\bar{\theta}}{32\pi^2} G_{\mu\nu}^A \tilde{G}^{A\mu\nu} \quad (1.3)$$

(where $\bar{\theta} = \theta + \arg(\det \mathcal{M})$ and where $G_{\mu\nu}^A$ is the gluon field strength tensor). Measurements of the neutron EDM require $\bar{\theta} \lesssim 10^{-10}$ which leads to the QCD naturalness problem (also known as the strong CP problem): why is this term - which should be present - so tiny? Peccei and Quinn [16] introduced an additional global PQ symmetry which is spontaneously broken at scale $v_{PQ} \sim 10^{10}$ GeV leading to a quasi-visible [17, 18] axion [19]. Introduction of the axion field allows the offending CP -violating term to dynamically settle to zero, thus saving the day for QCD. The required axion field ought to have a mass $m_a \sim 620 \mu\text{eV} \left(\frac{10^{10} \text{ GeV}}{f_a/N} \right)$ where N is the color anomaly of the PQ symmetry ($N = 1$ for KSVZ [17] and $N = 6$ for DFSZ [18]).

The axion can be produced via axion field coherent oscillations in the early universe and serves as a candidate for cold dark matter [20]. In a SUSY context, the axion should be accompanied by the spin-1/2 R -parity-odd axino \tilde{a} and the spin-0 R -even saxion field s . In supergravity models, the soft breaking saxion mass $m_s \sim m_{3/2}$. The axino mass is more model dependent [21, 22] but is usually also expected to be $m_{\tilde{a}} \sim m_{3/2}$. The axion, saxion and axino interactions are all suppressed by the inverse of the axion decay constant f_a where $f_a \sim v_{PQ}$.

1.3 Naturalness and the μ -problem

While the axion plays a crucial role in solving the QCD naturalness problem, it also plays a role in the electroweak naturalness problem. While the soft term $m_{H_u}^2$ can be radiatively driven to small negative values by the large top-quark Yukawa coupling, the μ parameter in Eq. 1.2 also needs to be tamed. Since it is supersymmetric and not SUSY breaking, naively one expects $\mu \sim m_{\text{GUT}}$ or M_P (the reduced Planck mass). In contrast, naturalness requires $\mu \sim m_{\text{weak}}$. The SUSY DFSZ axion provides an elegant resolution of this so-called SUSY μ problem [23] in that the Higgs superfields now carry PQ charge which forbids the appearance of the μ term in the superpotential. Upon spontaneous breaking of the PQ symmetry, then in the SUSY DFSZ axion model the μ term is regenerated with a value $\mu \sim \lambda_\mu f_a^2 / M_P$. This is in contrast to the SUSY soft terms which gain a mass $m_{\text{soft}} \sim m_{3/2} \sim m_{\text{hidden}}^2 / M_P$ where m_{hidden} is the hidden sector mass scale. In such a case, the emerging Little Hierarchy $\mu \ll m_{3/2}$ is just a consequence of a mismatch between hidden sector and PQ sector intermediate mass scales $f_a \ll m_{\text{hidden}}$. In fact, in models such as the MSY SUSY axion model [24], the PQ symmetry is broken radiatively as a consequence of SUSY breaking leading naturally to $\mu \sim 100 - 300$ GeV whilst $m_{3/2} \sim 2 - 10$ TeV [25]. As a by-product of radiative PQ breaking, intermediate scale Majorana masses are also induced $m_N \sim f_a$ leading to see-saw neutrinos [26]. In this scenario, then, the PQ breaking scale f_a plays a role in determining the axion, the higgsino and the Higgs masses!

1.4 Dark matter in SUSY with electroweak and QCD naturalness

In a highly natural model where the electroweak sector is stabilized by SUSY, the QCD sector is stabilized by the axion, the μ problem is resolved by PQ-charged Higgs fields and the Little Hierarchy $\mu \ll m_{3/2}$ emerges from radiative PQ breaking, then one expects dark matter to be composed of an axion-higgsino admixture: *i.e.* two dark matter particles. The favored axion scale $f_a \sim \sqrt{\mu M_P / \lambda_\mu} \sim 10^{10-12}$ GeV (for $\lambda_\mu \sim 0.01 - 1$) which is somewhat below the range of f_a currently being explored by the axion dark matter search experiment, ADMX [27]. Regarding the higgsino-like WIMPs, their relic abundance calculation is seriously modified from the usual thermal production picture [28]. To be sure, the WIMPs are still produced thermally, but they can also arise via axino and saxion production in the early universe, followed by cascade decays which terminate in WIMPs. While axinos can be produced thermally, saxions can be produced both thermally and via coherent oscillations. If too many WIMPs are produced via heavy particle decays, then they may undergo a re-annihilation process [29, 30]. Furthermore, axions can also be produced thermally or via saxion decays. The latter leads to injection of dark radiation parametrized by the effective number of additional neutrinos present in the cosmic soup: ΔN_{eff} . Current bounds from the Planck experiment require $N_{\text{eff}} = 3.15 \pm 0.23$ [31]. (To be conservative, here we require merely $\Delta N_{\text{eff}} \lesssim 1$ in our results.) With an assortment of interwoven production and decay processes occurring, an accurate estimate of the ultimate mixed axion-higgsino dark matter content requires simultaneous solution of eight coupled Boltzmann equations which track the abundance of radiation, WIMPs, thermal- and oscillation-produced axions, thermal- and oscillation-produced saxions, axinos and gravitinos [32].

Results vary radically depending on whether one is in a hadronic (KSVZ) [17] SUSY axion model or DFSZ [18] SUSY axion model. In the former KSVZ case, thermal production of axinos and saxions is proportional to the re-heat temperature T_R [33] while decay modes arise from heavy quark induced loop diagrams due to the superpotential term

$$W_{\text{KSVZ}} \ni m_Q e^{A/f_a} Q Q^c \quad (1.4)$$

where Q stands for intermediate-scale heavy quark superfields with $m_Q \sim f_a$. In SUSY DFSZ, axino and saxion thermal productions are different from those in SUSY KSVZ since the axion superfield has tree level couplings which are proportional to the SUSY μ parameter [34, 35, 36]:

$$W_{\text{DFSZ}} \ni \mu e^{-2A/f_a} H_u H_d. \quad (1.5)$$

Due to this interaction, thermal production of axions, axinos and saxions is largely independent of T_R unless $T_R \lesssim \mu$ [35]. Decays also dominantly proceed through this tree level coupling so the axino and saxion tend to be shorter-lived than in the KSVZ case.

1.5 Connection to baryogenesis

One of the major mysteries of particle physics and cosmology is the origin of the matter-anti-matter asymmetry as embodied by the measurement of the baryon-to-photon ratio [37]

$$\eta_B \equiv \frac{n_B}{n_\gamma} \simeq (6.2 \pm 0.5) \times 10^{-10} \quad (95\% \text{ CL}). \quad (1.6)$$

η_B is determined both from light element production in Big Bang Nucleosynthesis (BBN) and also from CMB measurements. Alternatively, this is sometimes expressed as the baryon-to-entropy ratio

$$\frac{n_B}{s} \simeq 10^{-10} \quad (1.7)$$

where $s \simeq 7.04n_\gamma$ in the present epoch.

Production of the baryon asymmetry of the Universe or BAU requires mechanisms which satisfy the three Sakharov criteria: 1. baryon number violation, 2. C and CP violation and 3. a departure from thermal equilibrium. Early proposals such as Planck scale or GUT scale baryogenesis seem no longer viable since the BAU would have been inflated away during the inflationary epoch of the Universe. Alternatively, most modern proposals for developing the BAU take place after the end of the inflationary epoch, at or after the era of re-heating which occurs around the re-heat temperature T_R . In fact, the SM contains all the ingredients for successful *electroweak* baryogenesis since baryon (and lepton) number violating processes can take place at large rates at high temperature $T > T_{\text{weak}} \sim 100$ GeV via sphaleron processes [38]. Unfortunately, these first order phase transition effects require a Higgs mass $\lesssim 50$ GeV, and so has been excluded for many years. By invoking supersymmetry, then new possibilities emerge for electroweak baryogenesis. However, successful SUSY electroweak baryogenesis seems to require a Higgs mass $m_h \lesssim 113$ GeV and a right-handed top-squark $m_{\tilde{t}_R} \lesssim 115$ GeV [39]. These limits can be relaxed to higher values so long as other sparticle/Higgs masses such as $m_A \gg 10$ TeV. Such heavy Higgs masses are not allowed if we stay true to our guidance from naturalness: after all, Eq. 1.2 requires $m_{H_d}^2/\tan^2\beta \lesssim m_Z^2/2$. For heavy Higgs masses, then $m_A \sim m_{H_d}$ and then from naturalness we find $m_A \lesssim 4 - 8$ TeV (depending on $\tan\beta$) [40].

In Sec. 2, we survey several leptogenesis mechanisms as the most promising baryogenesis mechanisms: 1. thermal leptogenesis [41, 42], 2. non-thermal leptogenesis via inflaton decay [44] 3. leptogenesis from oscillating sneutrino decay [45, 47] and 4. leptogenesis via an Affleck-Dine condensate [48, 49, 45].

Each of these processes requires some range of re-heat temperature T_R and gravitino mass $m_{3/2}$, and indeed some of them run into conflict with the so-called cosmological gravitino problem [50]. In this case, gravitinos can be thermally produced in the early universe at a rate proportional to T_R [51]. If T_R is too high then too much dark matter arises from thermal gravitino production followed by cascade decays to the LSP. Also, even if dark matter abundance constraints are respected, if the gravitino is too long-lived, then it may decay after the onset of BBN thus destroying the successful BBN predictions of the light element abundances [52, 53, 54].

In the case of natural SUSY with mixed axion-higgsino dark matter, then similar constraints arise from axino and saxion production: WIMPs or axions can be overproduced, or light element abundances can be destroyed by late decaying axinos and saxions. After a brief review of the several leptogenesis mechanisms in Sec. 2, in Sec. 3 we show constraints on leptogenesis in the T_R vs. $m_{3/2}$ planes assuming a natural SUSY spectrum. In Sec. 4, we show corresponding results in the T_R vs. f_a planes. We vary the PQ scale f_a from values favored by naturalness $f_a \sim 10^{10} - 10^{12}$ GeV to much higher values. While

thermal leptogenesis mechanism is quite constrained depending on $m_{3/2}$ and T_R , the latter three mechanisms appear plausible over a wide range of T_R , $m_{3/2}$ and f_a values which are consistent with naturalness. A summary and some conclusions are presented in Sec. 5.

2. Survey of some baryogenesis mechanisms

2.1 Thermal leptogenesis (THL)

Thermal leptogenesis [41, 42, 43] is a baryogenesis mechanism which relies on the introduction of three intermediate mass scale right hand singlet neutrinos N_i ($i = 1 - 3$) so that the (type I) see-saw mechanism [26] elegantly generates a very light spectrum of usual neutrino masses. The superpotential is given by

$$W \ni \frac{1}{2} M_i N_i N_i + h_{i\alpha} N_i L_\alpha H_u \quad (2.1)$$

where we assume a basis for the N_i masses which is diagonal and real. The index α denotes the lepton doublet generations and $h_{i\alpha}$ are the neutrino Yukawa couplings. From the see-saw mechanism, one expects a spectrum of three sub-eV mass Majorana neutrinos m_1 , m_2 and m_3 and three heavy neutrinos $M_1 < M_2 < M_3$ where in GUT-type theories one typically expects $M_3 \sim 10^{15}$ GeV. If the heavy neutrino masses are hierarchical (as assumed here) like the quark masses, then one might expect $M_1/M_3 \sim m_u/m_t \sim 10^{-5}$ and so perhaps $M_1 \sim 10^{10}$ GeV.

After inflation, then it is assumed the Universe re-heats to a temperature $T_R \gtrsim M_1$ thus creating a thermal population of N_1 s. The N_1 decay asymmetrically as $N_1 \rightarrow LH_u$ vs. $\bar{L}\bar{H}_u$ due to interference between tree and loop-level decay diagrams which include CP violating interactions. The CP asymmetry factor

$$\epsilon_1 \equiv \frac{\Gamma(N_1 \rightarrow LH_u) - \Gamma(N_1 \rightarrow \bar{L}\bar{H}_u)}{\Gamma_{N_1}} \quad (2.2)$$

is calculated to be [55]

$$\epsilon_1 \simeq \frac{3}{8\pi} \frac{M_1}{\langle H_u \rangle^2} m_{\nu_3} \delta_{\text{eff}} \quad (2.3)$$

where $\langle H_u \rangle \simeq 174 \text{ GeV} \sin \beta$ and δ_{eff} is an effective CP-violating phase which depends on the MNS matrix elements and which is expected to be $\delta_{\text{eff}} \sim 1$. For hierarchical heavy neutrinos, one expects

$$\epsilon_1 \sim 2 \times 10^{-10} \left(\frac{M_1}{10^6 \text{ GeV}} \right) \left(\frac{m_{\nu_3}}{0.05 \text{ eV}} \right) \delta_{\text{eff}}. \quad (2.4)$$

The ultimate lepton asymmetry requires evaluation via a coupled Boltzmann equation calculation [56]. The lepton-number-density to entropy ratio is given by

$$\frac{n_L}{s} = \kappa \epsilon_1 \frac{n_{N_1}}{s} = \kappa \frac{\epsilon_1}{240} \quad (2.5)$$

where the co-efficient κ accounts for washout effects and the efficiency of thermal N_1 production. Numerical evaluations of κ imply $\kappa \simeq 0.05 - 0.3$.

The induced lepton asymmetry becomes converted to a baryon asymmetry via B - and L - violating but $B - L$ conserving sphaleron interactions [38, 57]. The ultimate baryon asymmetry is given by [58]

$$\frac{n_B}{s} \simeq 0.35 \frac{n_L}{s} \simeq 0.3 \times 10^{-10} \left(\frac{\kappa}{0.1} \right) \left(\frac{M_1}{10^9 \text{ GeV}} \right) \left(\frac{m_{\nu_3}}{0.05 \text{ eV}} \right) \delta_{\text{eff}} \quad (2.6)$$

provided that T_R is large enough that the N_1 are efficiently produced by thermal interactions: $T_R \gtrsim M_1$. Naively, this requires $T_R \gtrsim 10^{10}$ GeV although detailed calculations [56] allow for $T_R \gtrsim 1.5 \times 10^9$ GeV. This rather large lower bound on T_R potentially leads to conflict with the gravitino problem and violation of BBN bounds or overproduction of dark matter. In the event that late-decaying relics inject entropy after N_1 decay is complete, then n_L/s is modified by an entropy-dilution factor r : $n_L/s \rightarrow n_L/rs$.

2.2 Non-thermal leptogenesis via inflaton decay (NTHL)

As an alternative to thermal leptogenesis, non-thermal leptogenesis posits a large branching fraction of the inflaton field χ into $N_1 N_1$: $\chi \rightarrow N_1 N_1$ which is followed by asymmetric N_1 decay to (anti-)leptons as before. In this case, the N_1 number-density-to-entropy-density ratio is given by [44, 59]

$$\frac{n_{N_1}}{s} \simeq \frac{\rho_{\text{rad}}}{s} \frac{n_\chi}{\rho_\chi} \frac{n_{N_1}}{n_\chi} \quad (2.7)$$

$$= \frac{3}{4} T_R \times \frac{1}{m_\chi} \times 2B_r = \frac{3}{2} B_r \frac{T_R}{m_\chi} \quad (2.8)$$

where ρ_{rad} is the radiation density once reheating has completed and ρ_χ is the energy density stored in the inflaton field just before inflaton decay. Thus, $\rho_{\text{rad}} \simeq \rho_\chi$ and $\rho_\chi \simeq m_\chi n_\chi$. Here also B_r is the inflaton branching fraction into $N_1 N_1$. The lepton-number-to-entropy ratio is then given by $n_L/s \simeq \epsilon_1 n_{N_1}/2$ where ϵ_1 is as in Eq. 2.3.

The lepton number asymmetry is converted to a baryon asymmetry via sphaleron interactions as before:

$$\frac{n_B}{s} \simeq 0.35 \frac{n_L}{s} \quad (2.9)$$

so that finally

$$\frac{n_B}{s} \simeq 0.5 \times 10^{-10} B_r \left(\frac{T_R}{10^6 \text{ GeV}} \right) \left(\frac{2M_1}{m_\chi} \right) \left(\frac{m_{\nu_3}}{0.05 \text{ eV}} \right) \delta_{\text{eff}} \quad (2.10)$$

where δ_{eff} is the same phase as given above. The resultant baryon asymmetry can match data provided $m_\chi > 2M_1$ and that the branching fraction is nearly maximal. Under these conditions, a re-heat temperature $T_R \gtrsim 10^6$ GeV is required. For $T_R \lesssim 10^6$ GeV, then ρ_{rad} and consequently ρ_χ are reduced so that there is insufficient energy stored in the inflaton field to generate the required n_{N_1} number density.

2.3 Leptogenesis from oscillating sneutrino decay (OSL)

In the previous two mechanisms, right-handed neutrinos and sneutrinos are produced by thermal scattering or inflaton decay. On the other hand, for right sneutrinos¹, coherent oscillation can be a dominant production process. The decay of oscillating sneutrino produces lepton asymmetry which is given by [47]

$$n_L = \epsilon_1 M_1 \left| \tilde{N}_{1d} \right|^2, \quad (2.11)$$

where \tilde{N}_{1d} is the sneutrino amplitude when it decays. The CP asymmetry factor ϵ_1 is the same as thermal leptogenesis which is shown in Eq. 2.3.

Once the universe is dominated by sneutrino oscillation, pre-existing relics are mostly diluted away and the universe is reheated again by sneutrino decay at $H = \Gamma_{N_1}$, where Γ_{N_1} is the sneutrino decay rate. The decay temperature T_{N_1} is determined by

$$T_{N_1} = \left(\frac{90}{\pi^2 g_*} \right)^{1/4} \sqrt{M_P \Gamma_{N_1}}, \quad (2.12)$$

while the entropy density is given by

$$s = \frac{2\pi^2}{45} g_* T_{N_1}^3, \quad (2.13)$$

where g_* is the number of degree of freedom at $T = T_{N_1}$. From these relations, one finds the lepton-number-to-entropy ratio:

$$\begin{aligned} \frac{n_L}{s} &= \frac{3}{4} \epsilon_1 \frac{T_{N_1}}{M_1} \\ &\simeq 1.5 \times 10^{-10} \left(\frac{T_{N_1}}{10^6 \text{ GeV}} \right) \left(\frac{m_{\nu 3}}{0.05 \text{ eV}} \right) \delta_{\text{eff}}. \end{aligned} \quad (2.14)$$

The baryon asymmetry is obtained via sphaleron process, and thus baryon number is given by

$$\frac{n_B}{s} \simeq 0.35 \frac{n_L}{s}. \quad (2.15)$$

Thus, enough baryon number can be generated for $T_{N_1} \gtrsim 10^6 \text{ GeV}$.

In this scenario, it is interesting that the effective reheat temperature is $\mathcal{O}(T_{N_1})$ for thermal relic particles, since sneutrino domination dilutes pre-existing particles when it decays [47].² Therefore, in the numerical analyses of Sec's. 3 and 4, we consider T_{N_1} a reheat temperature for production of gravitinos, axinos and saxions in the case of leptogenesis from oscillating sneutrino decay.

¹The spin-0 partners of right-hand neutrinos.

²It is assumed that inflaton decay after sneutrino oscillation starts. If sneutrino oscillation starts after inflaton decay, effective reheat temperature is given by $2T_{N_1}(T_R/T_{R_C})$ where T_{R_C} is the temperature at which sneutrino oscillation starts.

2.4 Affleck-Dine leptogenesis (ADL)

The last mechanism for baryogenesis is known as Affleck-Dine (AD) [48, 49] leptogenesis. AD leptogenesis makes use of the LH_u flat direction in the scalar potential [60, 49, 61]. This direction is lucrative in that it is not plagued by Q -balls which are problematic for flat directions carrying baryon number [62] and also because the rate for baryogenesis can be linked to the mass of the lightest neutrino, leading to a possible consistency check via observations of neutrinoless double beta decay ($0\nu\beta\beta$) [63].

In the case of the LH_u flat direction, F -flatness is only broken by higher dimensional operators which also give rise to neutrino mass via the see-saw mechanism [26]:

$$W \ni \frac{1}{2M_i}(L_i H_u)(L_i H_u) \quad (2.16)$$

where M_i is the heavy neutrino mass scale. The most efficient direction is that for which $i = 1$ corresponding to the lightest neutrino mass: $m_{\nu_1} \sim \langle H_u \rangle^2 / M_1$ in a basis where the neutrino mass matrix is diagonal. The Affleck-Dine field ϕ then occurs as

$$\tilde{L}_1 = \frac{1}{\sqrt{2}} \begin{pmatrix} \phi \\ 0 \end{pmatrix} \quad H_u = \frac{1}{\sqrt{2}} \begin{pmatrix} 0 \\ \phi \end{pmatrix}. \quad (2.17)$$

The scalar potential is given by

$$V = V_{SB} + V_H + V_{TH} + V_F \quad (2.18)$$

where

$$V_{SB} = m_\phi^2 |\phi|^2 + \frac{m_{\text{SUSY}}}{8M} (a_m \phi^4 + h.c.) \quad (2.19)$$

$$V_H = -c_H H^2 |\phi|^2 + \frac{H}{8M} (a_H \phi^4 + h.c.) \quad (2.20)$$

$$V_{TH} = \sum_{f_k |\phi| < T} c_k f_k^2 T^2 |\phi|^2 + \frac{9\alpha_s^2(T)}{8} T^4 \ln \left(\frac{|\phi|^2}{T^2} \right) \quad \text{and} \quad (2.21)$$

$$V_F = \frac{1}{4M^2} |\phi|^6. \quad (2.22)$$

The first contribution V_{SB} is the SUSY breaking contribution where $m_\phi^2 = (\mu^2 + m_{H_u}^2 + m_L^2)/2$ [64]. In natural SUSY, we expect $|\mu| \sim |m_{H_u}| \sim m_Z$ in contrast to $m_L \sim m_{\text{SUSY}} \sim 2 - 10$ TeV in accord with LHC8 limits.³ The second contribution arises from SUSY breaking during inflation [49] where $3H_I^2 m_{\text{GUT}}^2 \simeq |F_\chi|^2$ with H_I being the Hubble constant during inflation and where F_χ is the inflaton F -term which fuels inflation and χ is the inflaton field. In the expression V_H , the coefficient c_H may be > 0 for a non-flat Kahler metric (which is to be expected in general). This term provides an instability of the potential at $|\phi| = 0$ and for $c_H > 0$, then a large VEV of ϕ can form with value $\langle \phi \rangle \sim \sqrt{MH_I}$

³In gravity mediation, it is natural to have $m_{\text{SUSY}} \sim m_{3/2}$. In our benchmark study in Sec. 3, however, m_{SUSY} for SUSY particle spectrum is fixed while physical gravitino mass $m_{3/2}$ varies from 1 TeV to 100 TeV.

where $H_I \gg m_\phi$ and where $\arg(\phi) = [(-\arg(a_H) + (2n+1)\pi)/4]$ for $n = 0 - 3$. The second term in V_H is the Hubble-induced trilinear SUSY breaking term. The term V_F is the up-lifting F -term contribution arising from the higher-dimensional operator 2.16. Lastly, the term V_{TH} arises from thermal effects [65, 66]. The first term is generated when the light particle species which couple to the AD field are produced in the thermal plasma, while the second term is generated by effective gauge coupling running from heavy effective mass of particles which couple to the AD field. Here, f_k represents the Yukawa/gauge couplings of ϕ and c_k is expected ~ 1 .

The equation of motion for the AD field is given by

$$\ddot{\phi} + 3H\dot{\phi} + \frac{\partial V}{\partial \phi^*} = 0 \quad (2.23)$$

which is the usual equation for a damped harmonic oscillator. Once the AD condensate forms, then the universe continues expansion and the Hubble-induced terms decrease. The minimum of the potential decreases as does the value of the condensate. When H decreases to a value [67]

$$H_{\text{osc}} = \max \left[m_\phi, H_i, \alpha_2 T_R \left(\frac{9M_P}{8M} \right)^{1/2} \right] \quad (2.24)$$

(where $H_i = \min \left[\frac{1}{f_i^4} \frac{M_P T_R^2}{M^2}, (c_i^2 f_i^4 M_P T_R^2)^{1/3} \right]$) then the AD field begins to oscillate, and a non-zero lepton number arises: $n_L = \frac{i}{2}(\dot{\phi}^* \phi - \phi^* \dot{\phi})$ governed by

$$\dot{n}_L + 3Hn_L = \frac{m_{\text{SUSY}}}{2M} \text{Im}(a_m \phi^4) + \frac{H}{2M} \text{Im}(a_H \phi^4). \quad (2.25)$$

The first term on the RHS of Eq. 2.25 is dominant and using $d/dt(R^3 n_L) = R^3 \dot{n}_L + 3R^3 H n_L$ we can integrate from early times up to $t = 1/H_{\text{osc}}$ to find

$$n_L = \frac{m_{\text{SUSY}}}{2M} \text{Im}(a_m \phi^4) t_{\text{osc}} \quad (2.26)$$

where $t_{\text{osc}} = 2/3H_{\text{osc}}$ for an oscillating field/matter-dominated universe. The lepton-number-to-entropy ratio is assumed conserved once the era of re-heat is completed:

$$\frac{n_L}{s} = \frac{M T_R}{12M_P^2} \left(\frac{m_{\text{SUSY}}}{H_{\text{osc}}} \right) \delta_{\text{eff}}. \quad (2.27)$$

This quantity has the virtue of being T_R independent if H_{osc} is determined by the third (thermal) contribution in Eq. 2.24 [67]. The lepton asymmetry is then converted to a baryon asymmetry via sphaleron interactions

$$\frac{n_B}{s} \simeq 0.35 \frac{n_L}{s}. \quad (2.28)$$

Replacing M by $\langle H_u \rangle^2 / m_{\nu_1}$, then it is found [67] that a baryon-to-entropy ratio $n_B/s \sim 10^{-10}$ can be developed roughly independent of T_R for $T_R \gtrsim 10^5$ GeV for $m_{\nu_1} \sim 10^{-8}$ eV and for $m_{\text{SUSY}} \sim 10$ TeV.

3. Constraints in the T_R vs. $m_{3/2}$ plane for various f_a

To compute the mixed axion-WIMP dark matter abundance in SUSY axion models, we adopt the eight-coupled Boltzmann equation computation of Ref's [68, 69, 32]. In that treatment, one begins at temperature $T = T_R$ and tracks the energy densities of radiation, WIMPs, gravitinos, axinos, saxions (CO- and thermally-produced) and axions (CO-, thermally- and saxion decay-produced). Whereas WIMPs quickly reach thermal equilibrium at $T = T_R$, the axinos, saxions, axions and gravitinos do not, even though they are still produced thermally. In SUSY KSVZ, the axino, axion and saxion thermal production rates are all proportional to T_R [33] while in SUSY DFSZ model they are largely independent of T_R [35]. The calculation depends sensitively on the sparticle mass spectrum, on the re-heat temperature T_R , on the gravitino mass $m_{3/2}$ and on the PQ model (KSVZ or DFSZ), the PQ parameters f_a , the axion mis-alignment angle θ_i , the saxion angle θ_s (where the initial saxion field value is given as $s = \theta_s f_a$) and on a parameter ξ_s which accounts for the model-dependent saxion-to-axion coupling [21]. Here, we adopt the choices $\xi_s = 0$ ($s \rightarrow aa$, $\tilde{a}\tilde{a}$ decays turned off) or $\xi_s = 1$ ($s \rightarrow aa$, $\tilde{a}\tilde{a}$ decays turned on).

The calculation depends sensitively on the axino, saxion and gravitino decay rates. The gravitino decay rates are adopted from Ref. [70] while the axino and saxion decay rates are given in Ref's [30, 71] for SUSY KSVZ and in Ref. [72] for SUSY DFSZ. The axino decays via loops involving the heavy quark Q field such that $\tilde{a} \rightarrow g\tilde{g}$, $\tilde{Z}_i\gamma$ and $\tilde{Z}_i Z$ in SUSY KSVZ. In SUSY DFSZ, the axino couples directly to Higgs superfields yielding faster decay rates into gauge/Higgs boson plus gaugino/higgsino states. In SUSY KSVZ, the saxion decays via $s \rightarrow gg$, $\tilde{g}\tilde{g}$ and, when $\xi_s = 1$, also to aa and $\tilde{a}\tilde{a}$ (if kinematically allowed). The decay $s \rightarrow aa$ leads to production of dark radiation as parametrized by ΔN_{eff} . In SUSY DFSZ, the saxion decays directly to gauge- or Higgs-boson pairs or to gaugino/higgsino pairs [72]. If $\xi_s = 1$, then also $s \rightarrow aa$ or $\tilde{a}\tilde{a}$. In the case where axinos or saxions decay to SUSY particles (leading to WIMPs), then WIMPs may re-annihilate.

For the SUSY mass spectrum, we generate a natural SUSY model within the context of the 2-extra parameter non-universal Higgs (NUHM2) model with $m_0 = 5$ TeV, $m_{1/2} = 0.7$ TeV, $A_0 = -8.4$ TeV and $\tan\beta = 10$. We take $\mu = 125$ GeV and $m_A = 1$ TeV. The spectrum is generated using IsaSUGRA 7.84 [73]. The value of $m_{\tilde{g}} = 1.8$ TeV so the model is safely beyond LHC8 constraints. The value of $m_h = 125$ GeV and $\Delta_{\text{EW}} = 20$ so the model is highly natural. Higgsino-like WIMPs with mass $m_{\tilde{Z}_1} = 115.5$ GeV are thermally underproduced so that $\Omega_{\tilde{Z}_1}^{\text{TP}} h^2 = 0.007$ using IsaReD [74]. In all frames, we take $m_{\tilde{a}} = m_s = m_{3/2}$ as is roughly expected in gravity-mediated SUSY breaking models [21, 22]. Since we take $m_{\tilde{a}} = m_s$, then $s \rightarrow \tilde{a}\tilde{a}$ decays are never a factor in our results.

In all plots, the light-blue region corresponds to the parameter space where all BBN, DM and dark radiation constraints are satisfied. The red region corresponds to BBN excluded region, gray to overproduction of dark matter and brown to $\Delta N_{\text{eff}} > 1$. Red and brown solid lines show the boundaries of excluded regions due to BBN and dark radiation respectively.

3.1 SUSY DFSZ model

Our first results of allowed regions in the T_R vs $m_{3/2}$ plane are shown in Fig. 1. In frame a), we first take $f_a = 10^{11}$ GeV and 10^{12} GeV and show allowed and excluded regions. For lower values of f_a , DM density is enhanced by gravitino decay only and BBN constraints are violated by late-decaying gravitinos since axinos and saxions are short-lived. For $f_a < 10^{11}$ GeV, BBN bounds and DM exclusion contours can be read from Fig. 1 once the region $T_R > f_a$ is omitted. As we increase f_a to 10^{11} GeV, then the axino and saxion decay rates are suppressed and they decay later. However, they still typically decay before neutralino freeze-out and thus do not change the picture.

The gray band at the top of frame a) is forbidden due to overproduction of WIMP dark matter due to thermal gravitino production and decay well after WIMP freeze-out. This occurs for $T_R \gtrsim 3 \times 10^{10}$ GeV when $f_a = 10^{11}$. The red-shaded region occurs due to violation of BBN constraints on late-decaying neutral relics. In the case of frame a), this comes again from gravitino production along with decay after the onset of BBN. Here, we use a digitized version of BBN constraints from Jedamzik [54] which appear in the $\Omega_X h^2$ vs. τ_X plane where X stands for the quasi-stable neutral particle, $\Omega_X h^2$ is its would-be relic abundance had it not decayed and τ_X is its lifetime. The curves also depend on the X -particle hadronic branching fraction B_h and on the mass m_X . Ref. [54] presents results for $m_X = 0.1$ and 1 TeV and we extrapolate between and beyond these values for alternative mass cases. Together, the red- and gray-shaded regions constitute the well-known *gravitino problem*: thermal gravitino production, which is proportional to T_R [51], can lead to overproduction of decay-produced WIMPs or violations of BBN constraints.

In comparison, we also show several lines. The black vertical lines show the constraint from naturalness ($\Delta_{EW} < 30$) that arises on m_0 in the NUHM2 model (labelled “RNS” at $m_{3/2} = 10$ TeV for universal generations and “RNS SF” at $m_{3/2} = 20$ TeV for split families [9]). Here, we assume $m_{\tilde{q}} \simeq m_{3/2}$ where the gravitino mass sets the matter scalar mass scale most directly in gravity-mediated SUSY breaking models.⁴ In addition, we show the regions where various leptogenesis mechanisms can account for the BAU. The region above $T_R = 1.5 \times 10^9$ GeV is where thermal leptogenesis (THL) can occur. From the plot, we see the viable region, colored as light-blue, is bounded by $m_{3/2} \gtrsim 5$ TeV by BBN, by $m_{3/2} \lesssim 10$ TeV by naturalness and by 1.5×10^9 GeV $< T_R < 5 \times 10^9$ GeV by BBN and by successful baryogenesis. Thus, THL is viable only in a highly restricted region of parameter space. In contrast, non-thermal leptogenesis (NTHL) and sneutrino leptogenesis (OSL) are viable in a much larger region bounded from below by $T_R \gtrsim 10^6$ GeV while Affleck-Dine LH_u flat-direction leptogenesis (ADL) is viable in an even larger region for $T_R \gtrsim 10^5$ GeV. These latter three leptogenesis regions are fully viable for $m_{3/2} > 1$ TeV.

⁴In the numerical scans, the SUSY spectrum is fixed as we discussed in the beginning of this section. However, even if the scalar masses differ from the fixed benchmark values as the gravitino varies, dark matter and baryogenesis do not change significantly. Thus, this argument remains correct for this reason.

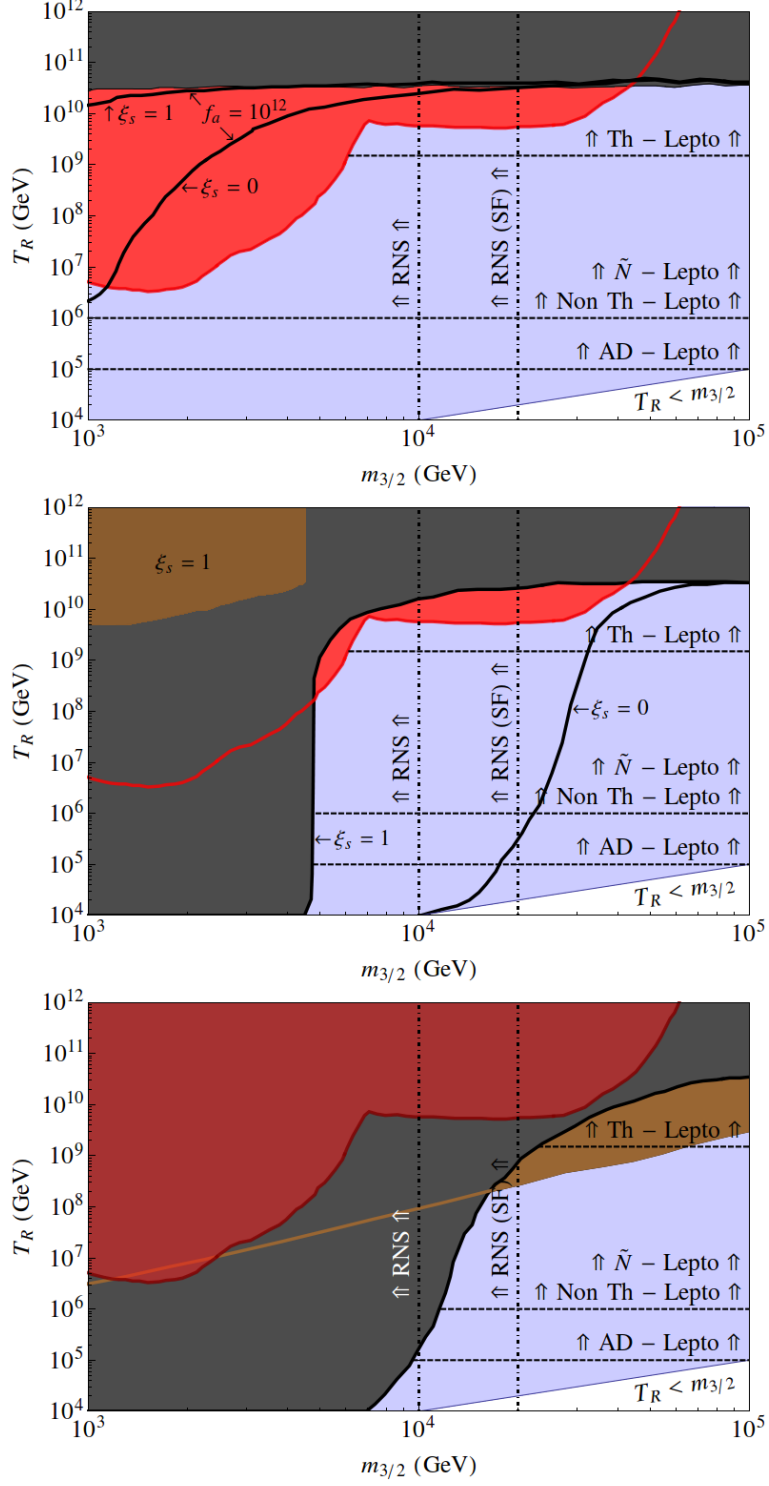


Figure 1: Plot of allowed regions in T_R vs. $m_{3/2}$ plane in the SUSY DFSZ axion model for a) $f_a = 10^{11}$ and 10^{12} GeV, b) $f_a = 10^{13}$ GeV, for $\xi_s = 0$ and 1 and c) $f_a = 10^{14}$ GeV for $\xi_s = 1$. For $f_a = 10^{11}$, $T_R > 10^{11}$ is forbidden to avoid PQ symmetry restoration. We take $m_s = m_{\bar{a}} \equiv m_{3/2}$ in all plots.

As f_a is increased to 10^{12} GeV, then decays of axino and saxion are suppressed even further. In this case, the DM-excluded region expands to the black contours labelled by $f_a = 10^{12}$ GeV and $\xi_s = 0$ or 1. The $\xi_s = 1$ region is smaller than the $\xi_s = 0$ region because for $\xi_s = 1$ the saxion decay width increases due to $s \rightarrow aa$ and the saxion lifetime is quicker. The important point is that SUSY electroweak naturalness expects $f_a \sim \sqrt{\mu M_P / \lambda_\mu} \sim 10^{10} - 10^{12}$ GeV and for these values then there are wide swaths of parameter space which support NTHL, OSL and ADL, and even THL is viable in some small region.

Instead, if we increase f_a to $\sim 10^{13}$ GeV as in frame *b*), then we are somewhat beyond the natural value of f_a , but also now the DM-forbidden region has increased greatly so that only values of $m_{3/2} \gtrsim 5$ TeV are allowed for $\xi_s = 1$, while for $\xi_s = 0$ then *all* of natural SUSY parameter space is forbidden. For low values of $m_{3/2}$ ($= m_s \Rightarrow$ long-lived saxions) and at high T_R , the decay $s \rightarrow aa$ produces too much dark radiation for $\xi_s = 1$ case only. This region is colored brown and triply excluded by DM, BBN and dark radiation constraints. In frame *c*), with $f_a = 10^{14}$ GeV, then natural SUSY parameter space is mostly forbidden by overproduction of WIMPs for $\xi_s = 1$ and totally forbidden for $\xi_s = 0$ (not shown in the Fig. 1c). In addition, the brown-shaded region ($\Delta N_{\text{eff}} > 1$) has extended and imposes an additional excluded region for $m_{3/2} \gtrsim 15$ TeV and $T_R \gtrsim 10^8$ GeV.

These results have important implications for axion detection. Currently, the ADMX experiment is exploring regions of $f_a/N_{\text{DW}} \gtrsim 10^{12}$ GeV (N_{DW} is domain wall number). Future plans include an exploration of regions down to $f_a/N_{\text{DW}} \gtrsim 10^{11}$ GeV. To make a complete exploration of the expected locus of the axion in natural SUSY, then such experiments should also aim for exploration down to $f_a/N_{\text{DW}} \sim 10^{10}$ GeV. For even smaller $f_a/N_{\text{DW}} < 10^{10}$ GeV values, then axion CO-production requires θ_i values very close to π and the axion production rates would be considered as fine-tuned [75].

3.2 SUSY KSVZ model

In this subsection, we show baryogenesis-allowed regions in the T_R vs. $m_{3/2}$ plane for the SUSY KSVZ model. We regard the SUSY KSVZ model as less lucrative in that one loses the DFSZ solution to the SUSY μ problem and the connection with electroweak naturalness. In addition, if the exotic heavy quark field Q is not an element of a complete GUT multiplet, then one loses gauge coupling unification. Nonetheless, it is instructive to view these results for comparison to the SUSY DFSZ case.

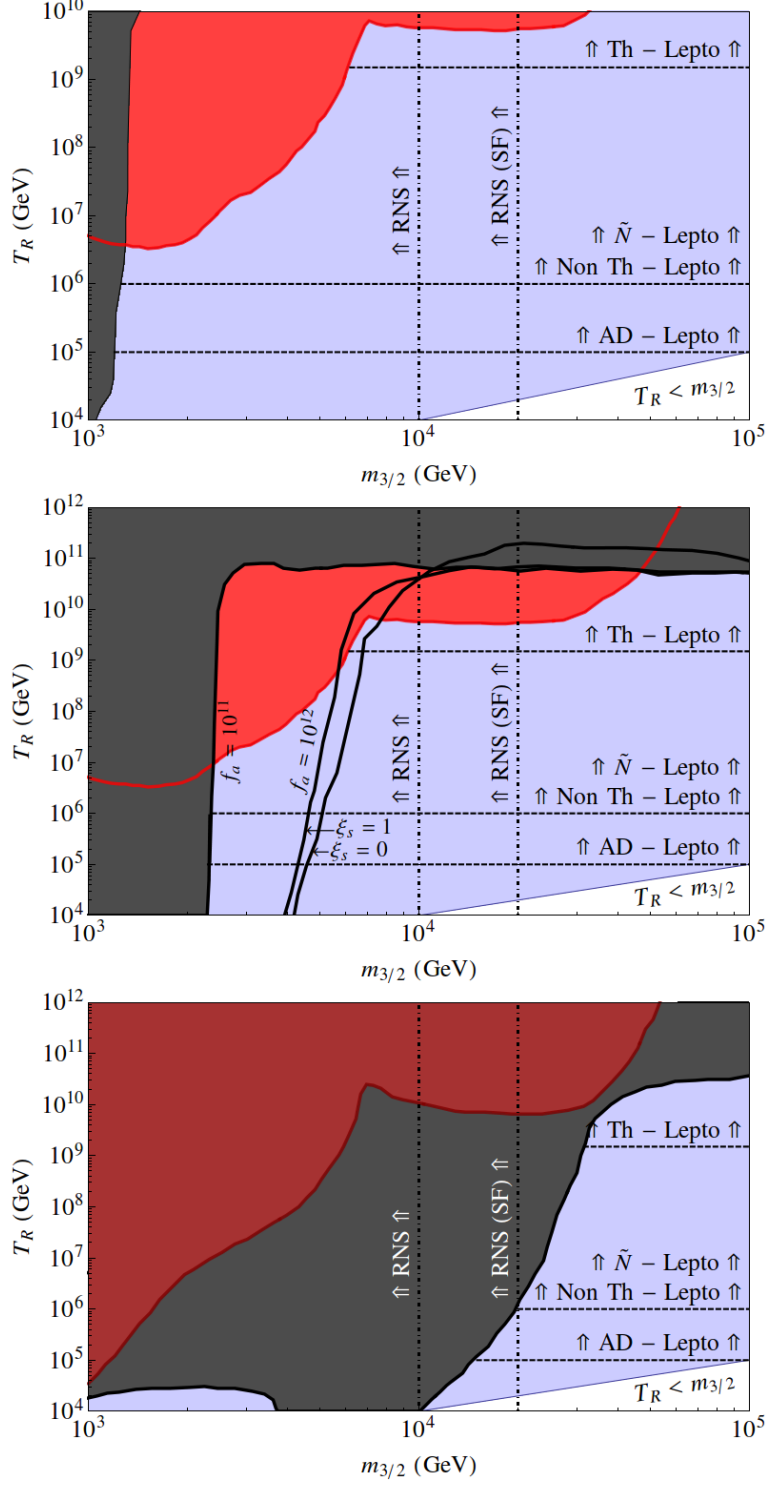


Figure 2: Plot of allowed regions in T_R vs. $m_{3/2}$ plane in the SUSY KSVZ axion model for a) $f_a = 10^{10}$ GeV, b) 10^{11} and 10^{12} GeV for $\xi_s = 0$ and 1 and c) $f_a = 10^{13}$ GeV for $\xi_s = 0$. For $f_a = 10^{11}$, $T_R > 10^{11}$ is forbidden to avoid PQ symmetry restoration. We take $m_s = m_{\bar{a}} = m_{3/2}$ in all plots.

In Fig. 2a), we show results for $f_a = 10^{10}$ GeV. Even for f_a as low as 10^{10} GeV, the gray-shaded WIMP-overproduction region occupies the region with $m_{3/2} \lesssim 1.3$ TeV. In this region, since $m_{\tilde{a}} \simeq m_{3/2}$, then thermal axino production followed by decay after neutralino freeze-out leads to WIMP over production across a wide range of T_R values. This is because the axino decay is suppressed by Q -mediated loops as compared to SUSY DFSZ. As f_a is increased to 10^{11} GeV (Fig. 2b)), then the DM-forbidden region expands out to $m_{3/2} \sim 2$ TeV region. For $f_a = 10^{12}$ GeV (Fig. 2b)), then the DM-forbidden region expands out to $m_{3/2} \sim 4$ TeV. Even for this high value of f_a , there is still room for leptogenesis in natural SUSY models for each of the cases of THL, NTHL, OSL and ADL.⁵

For the SUSY KSVZ model with $f_a = 10^{13}$ GeV as shown in Fig. 2c), then the DM-forbidden region has expanded to exclude all viable natural SUSY parameter space except for a tiny slice with $m_{3/2} \sim 15-20$ TeV and $T_R < 10^6$ GeV where ADL might still function.

4. Constraints in the T_R vs. f_a plane for fixed $m_{3/2}$

In this section, we examine the DM constraints on baryogenesis in the T_R vs. f_a plane for fixed natural $m_{3/2}$ values to gain further insights on axion decay constant dependence of the constraints for T_R between $10^4 - 10^{12}$ GeV. On these planes, in the yellow region labelled $T_R > f_a$ we expect PQ symmetry to be restored during reheating which leads to generation of separate domains with different θ values and the appearance of domain walls and associated problems. In this case, axion coherent oscillations must be averaged over separate domains [20]. As before, we do not consider this region.

4.1 SUSY DFSZ model

In Fig. 3, we plot allowed and forbidden regions for baryogenesis in SUSY DFSZ model in the T_R vs. f_a plane for $m_{3/2} = 5$ TeV. In frame a), with $\xi_s = 0$, the gray-shaded region still corresponds to WIMP overproduction and sets an upper limit of $f_a \lesssim 10^{12}$ GeV. The red-shaded region corresponds to violation of BBN constraints from late decaying gravitinos and bounds T_R from above: $T_R \lesssim 2 \times 10^8$ GeV which excludes the possibility of THL. Still, large regions of natural SUSY parameter space are consistent with NTHL, OSL and with ADL. The BBN bound kicks in again at $f_a \sim 6 \times 10^{14}$ due to long-lived saxions. For the case of $\xi_s = 1$ shown in Fig. 3b), then $s \rightarrow aa$ is turned on. This leads to the brown dark-radiation excluded region at very large f_a values and large T_R . In addition, we note for this case that the red-shaded BBN forbidden region has actually expanded compared to frame a). This is because for $\xi_s = 0$, the CO-produced saxions inject considerable entropy into the cosmic soup at large f_a thus diluting the gravitino abundance. For $\xi_s = 1$, then the saxion decays more quickly leading to less entropy dilution of gravitinos and thus more restrictive BBN bounds. Thus, the BBN constraints are actually more severe for $\xi_s = 1$. In addition, for frame b), we see WIMP overproduction bounds are less severe

⁵For this case only, we have found that there exists some mild entropy dilution r of n_L due to thermal axino production for $T_R \sim 10^{10} - 10^{11}$ GeV by up to a factor of 2. Since these T_R values are beyond the lower limit, our plots hardly change. Alternatively, the THL lower bound on T_R may be interpreted as a lower bound on T_R/r .

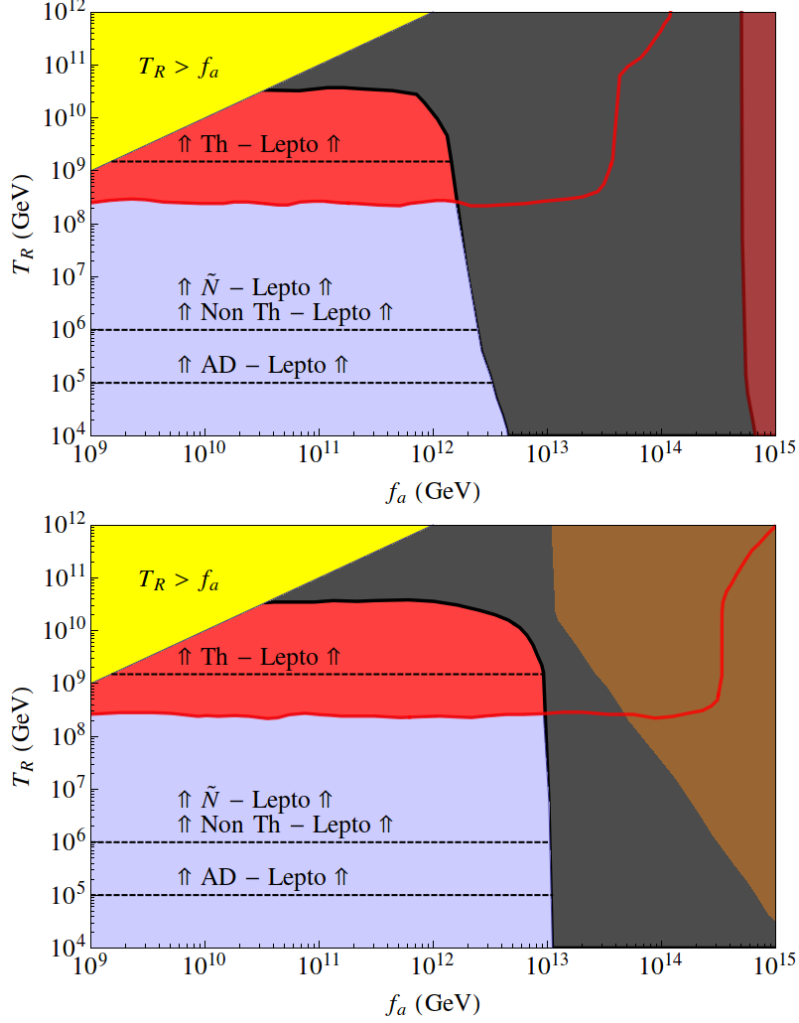


Figure 3: Plot of allowed regions in T_R vs. f_a plane in the SUSY DFSZ axion model for $m_{3/2} = 5$ TeV and with a) $\xi_s = 0$ and b) $\xi_s = 1$. We take $m_s = m_{\bar{a}} = m_{3/2}$ in all plots.

with $f_a \lesssim 10^{13}$ GeV being required for the allowed regions. These are due to a reduced $s \rightarrow SUSY$ branching fractions for the $\xi_s = 1$ case.

In Fig. 4 we show allowed and excluded regions in the T_R vs. f_a plane for $m_{3/2} = 10$ TeV. In the case of $\xi_s = 0$ shown in frame a), the larger gravitino mass causes the gravitinos to decay more quickly so that BBN constraints are diminished: in this case, the THL scenario with $T_R > 1.5 \times 10^9$ GeV is allowed in contrast to the previous case with $m_{3/2} = 5$ TeV. In addition, broad swaths of parameter space are allowed for the NTHL, OSL and ADL scenarios with $f_a \lesssim 5 \times 10^{12}$ GeV. For larger f_a values, then axino and saxion production followed by late decays leads to too much WIMP dark matter. For the case with $\xi_s = 1$ shown in frame b), we see again the BBN constraints are somewhat enhanced due to diminished entropy dilution of gravitinos at large f_a . In addition, a dark-radiation forbidden region has appeared. Most importantly, the DM-allowed region occurs

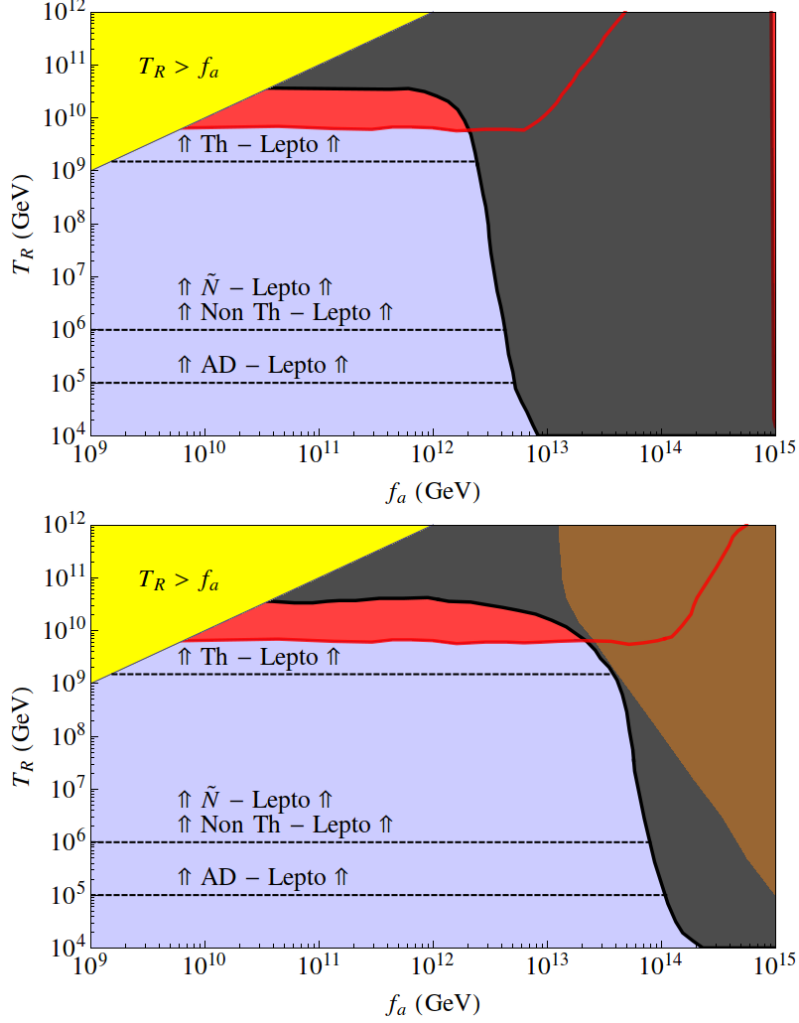


Figure 4: Plot of allowed regions in T_R vs. f_a plane in the SUSY DFSZ axion model for $m_{3/2} = 10$ TeV and with a) $\xi_s = 0$ and b) $\xi_s = 1$.

for $f_a \lesssim 10^{14}$ GeV so that large swaths of parameter space are open for baryogenesis. This is because, since we take $m_{\tilde{a}} = m_s = m_{3/2}$, then the axinos and saxions are also shorter-lived and tend to decay earlier - frequently before WIMP freeze-out - so DM overproduction is more easily avoided.

For even larger values of $m_{3/2}$ up to $m_{3/2} \sim 25$ TeV, we would expect to see a very similar BBN constraint since BBN bounds are not sensitive to any changes in $m_{3/2}$ for $7 \text{ TeV} \lesssim m_{3/2} \lesssim 25 \text{ TeV}$ (see Fig. 1). As $m_{3/2}$ increases and reaches beyond $m_{3/2} \sim 65$ TeV, then gravitino decays much sooner and does not violate BBN constraints at all. However DM production highly depends on f_a and the DM exclusion picture would look different up to a maximum f_a after which the whole parameter space is excluded by too much DM.

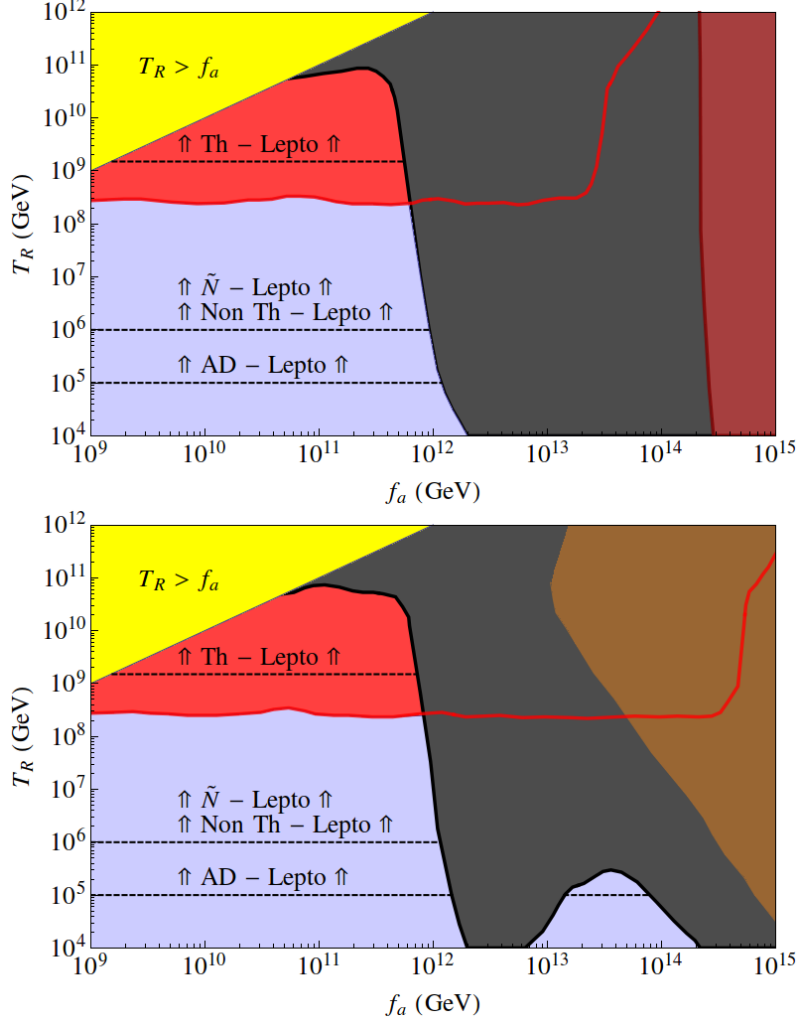


Figure 5: Plot of allowed regions in T_R vs. f_a plane in the SUSY KSVZ axion model for $m_{3/2} = 5$ TeV and with a) $\xi_s = 0$ and b) $\xi_s = 1$.

4.2 SUSY KSVZ model

In this subsection, we show corresponding results in the T_R vs. f_a plane for SUSY KSVZ. In Fig. 5 we show the plane for $m_{3/2} = 5$ TeV and a) $\xi_s = 0$. Here, we see that THL is ruled out due to the severe BBN bounds arising from gravitino production and decay which restrict $T_R \lesssim 2 \times 10^8$ GeV while the DM restriction rules out $f_a \gtrsim 10^{12}$ GeV. The NTHL, OSL and ADL are still viable baryogenesis mechanisms over a wide range of T_R and f_a values. In frame 5b) for $\xi_s = 1$, the DM forbidden region is similar with a $f_a < 10^{12}$ GeV restriction. However, the BBN restricted region has increased because there is less entropy dilution from saxion decay of the gravitinos abundance. The expanded BBN region lies in the already DM and dark radiation excluded region so provides no additional constraint. Since saxions decay earlier for $\xi_s = 1$ compared to $\xi_s = 0$, then they inject neutralinos at a higher decay temperature T_s^D ; as a consequence, a small DM-allowed region appears at

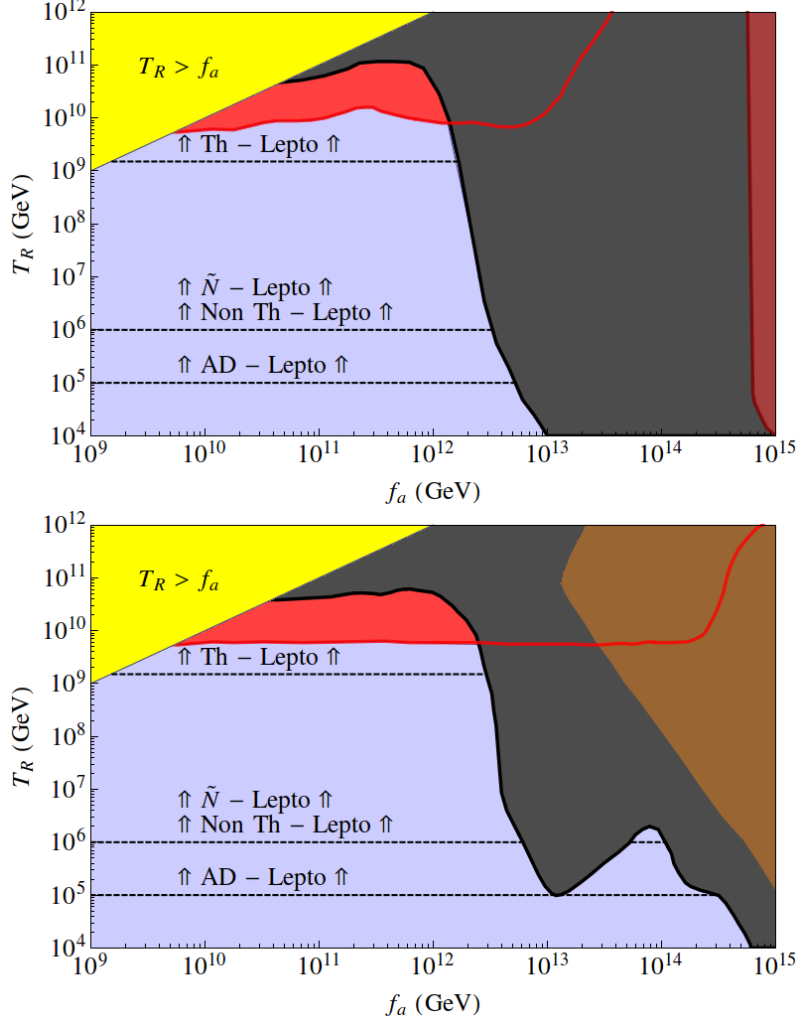


Figure 6: Plot of allowed regions in T_R vs. f_a plane in the SUSY KSVZ axion model for $m_{3/2} = 10$ TeV and with a) $\xi_s = 0$ and b) $\xi_s = 1$.

high $f_a \sim 10^{13} - 10^{14}$ GeV and $T_R \sim 10^5$ GeV which is barely consistent with ADL. In Fig. 6a), we show the same T_R vs. f_a plane with $\xi_s = 0$, but this time for a heavier value of $m_{3/2} = m_s = m_{\tilde{a}} = 10$ TeV. The higher value of $m_{3/2}$ means gravitinos decay more quickly and at higher temperature so that the BBN bound on T_R is given by $T_R \gtrsim 4 \times 10^9$ so that THL is again viable. Also, the DM-allowed region has moved to a higher f_a bound of $f_a \lesssim 2 \times 10^{12}$ GeV. In this frame, all four baryogenesis mechanisms are possible. In Fig. 6b), we show the same plane for $\xi_s = 1$. Here a prominent dark radiation excluded region appears at large $f_a \gtrsim 10^{13} - 10^{14}$ GeV, although this region is already excluded by WIMP overproduction and by BBN. The larger saxion width arising from the additional $s \rightarrow aa$ decay mode means the saxion decay at higher temperatures leading to some possible allowed regions appearing at $f_a \sim 10^{14}$ GeV and $T_R \sim 10^5$ GeV which admits ADL. Otherwise, large regions of viable parameter space exists for $f_a \lesssim 2 \times 10^{12}$ GeV and for $T_R \lesssim 4 \times 10^9$

GeV where all four leptogenesis mechanisms are possible.

5. Conclusion

In this paper we have investigated constraints on four compelling baryogenesis-via-leptogenesis scenarios within the framework of supersymmetric models with radiatively-driven naturalness. These models are especially attractive since they contain solutions to the gauge hierarchy problem (via SUSY), the strong CP problem (via the axion), the SUSY μ problem (for the case of the SUSY DFSZ axion) and the Little Hierarchy problem (where $\mu \sim 100 - 200$ GeV is generated from multi-TeV values of $m_{3/2}$). The characteristic, unambiguous signature of such models is the presence of light higgsinos $\tilde{Z}_{1,2}$ and \tilde{W}_1^\pm with mass $\sim \mu$. In these models, the LSP is a higgsino-like WIMP which is thermally underproduced. The remainder of the dark matter abundance is filled by the axion. Indeed, over most of parameter space the axion forms the bulk of dark matter [76].

In supersymmetric dark matter models, then baryogenesis mechanisms are confronted by the gravitino problem: gravitinos which are thermally produced in the early universe can lead to overproduction of WIMPs or to violations of BBN constraints. In SUSY axion models, there are analogous problems arising from thermal axino production and decay and from thermal- and oscillation-produced saxions. We calculated regions of the T_R vs. $m_{3/2}$ plane in the compelling RNS SUSY model with DFSZ axions and $\xi_s = 0$ and 1. Our main result is that the region of parameter space preferred by naturalness with $f_a \sim \sqrt{\mu M_P / \lambda_\mu} \sim 10^{10} - 10^{12}$ GeV supports all four leptogenesis mechanisms. The thermal leptogenesis is perhaps less plausible since its allowed region is nestled typically between the constricted region of $7 \text{ TeV} < m_{3/2} < 10 \text{ TeV}$ (or $< 20 \text{ TeV}$ in RNS for split families) and $1.5 \times 10^9 \text{ GeV} < T_R < 4 \times 10^9 \text{ GeV}$. The other NTHL, OSL and ADL mechanisms can freely operate over a broad region of parameter space for $f_a \lesssim 10^{12}$ GeV and $T_R \gtrsim 10^5$ GeV. We also evaluated all constraints in the T_R vs. f_a plane for fixed $m_{3/2} = 5$ and 10 TeV.

The broad allowed regions of parameter space basically favor the following.

- Multi-TeV values of $m_{3/2}$ to avoid BBN constraints and to hasten saxion and axino decays. Since $m_{3/2}$ sets the scale for superpartner masses at LHC, these multi-TeV values of $m_{3/2}$ are also supported by LHC8 sparticle search constraints and the large value of $m_h \sim 125$ GeV at little cost to naturalness.
- A value of $f_a \sim 10^{10} - 10^{12}$ GeV which suppresses WIMP over production from axino/saxion production. Such values of f_a lead to axion masses somewhat above the standard search region of ADMX and should motivate future axion search experiments to increase their search region to heavier axion masses.
- Values of $T_R \sim 10^5 - 10^9$ GeV.

For completeness, we have also evaluated the leptogenesis allowed regions in the SUSY KSVZ model for which an alternative solution to the μ problem is needed. The loop-suppressed axino and saxion decay rates typically lead to more stringent constraints in this

case although regions of parameter space can still be found where the various leptogenesis mechanisms are still possible.

Acknowledgments

We thank Vernon Barger for discussions and Andre Lessa for earlier collaborations on these topics. This work was supported in part by the US Department of Energy, Office of High Energy Physics. The computing for this project was performed at the OU Supercomputing Center for Education & Research (OSCER) at the University of Oklahoma (OU). KJB is also supported by Grant-in-Aid for Scientific research No. 26104009.

References

- [1] G. Aad *et al.* [ATLAS Collaboration], Phys. Lett. B **716**, 1 (2012).
- [2] S. Chatrchyan *et al.* [CMS Collaboration], Phys. Lett. B **716**, 30 (2012).
- [3] M. S. Carena and H. E. Haber, Prog. Part. Nucl. Phys. **50**,63 (2003).
- [4] G. Aad *et al.* [ATLAS Collaboration], JHEP **1409** (2014) 176; G. Aad *et al.* [ATLAS Collaboration], JHEP **1504** (2015) 116.
- [5] CMS Collaboration [CMS Collaboration], CMS-PAS-SUS-12-016.
- [6] H. Baer, V. Barger and A. Mustafayev, Phys. Rev. D **85** (2012) 075010.
- [7] A. Arbey, M. Battaglia, A. Djouadi, F. Mahmoudi and J. Quevillon, Phys. Lett. B **708** (2012) 162.
- [8] M. Shifman, Mod. Phys. Lett. A **27** (2012) 1230043; R. Barbieri, Phys. Scripta T **158** (2013) 014006; G. F. Giudice, PoS EPS -**HEP2013** (2013) 163; G. Altarelli, EPJ Web Conf. **71** (2014) 00005; N. Craig, arXiv:1309.0528 [hep-ph]; H. Murayama, Phys. Scripta T **158** (2013) 014025; G. G. Ross, Eur. Phys. J. C **74** (2014) 2699; J. Lykken and M. Spiropulu, Sci. Am. **310N5**, no. 5, 36 (2014); M. Dine, arXiv:1501.01035 [hep-ph].
- [9] H. Baer, V. Barger, P. Huang, A. Mustafayev and X. Tata, Phys. Rev. Lett. **109**, 161802 (2012); H. Baer, V. Barger, P. Huang, D. Mickelson, A. Mustafayev and X. Tata, Phys. Rev. D **87**, 115028 (2013).
- [10] H. Baer, V. Barger and M. Savoy, arXiv:1509.02929 [hep-ph].
- [11] H. Baer, V. Barger and D. Mickelson, Phys. Rev. D **88**, 095013 (2013).
- [12] H. Baer, V. Barger, D. Mickelson and M. Padeffke-Kirkland, Phys. Rev. D **89**, 115019 (2014).
- [13] J. R. Ellis, K. Enqvist, D. V. Nanopoulos and F. Zwirner, Mod. Phys. Lett. A **1** (1986) 57.
- [14] R. Barbieri and G. Giudice, *Nucl. Phys.* **B 306** (1988) 63.
- [15] S. Weinberg, Phys. Rev. D **11**, 3583 (1975).
- [16] R. D. Peccei and H. R. Quinn, Phys. Rev. Lett. **38**, 1440 (1977).
- [17] J. E. Kim, Phys. Rev. Lett. **43**, 103 (1979); M. A. Shifman, A. Vainstein and V. I. Zakharov, Nucl. Phys. B **166**, 493(1980).

- [18] M. Dine, W. Fischler and M. Srednicki, Phys. Lett. **B104** (1981) 199; A. P. Zhitnitskii, Sov. J. Phys. **31** (1980) 260.
- [19] S. Weinberg, Phys. Rev. Lett. **40**, 223 (1978); F. Wilczek, Phys. Rev. Lett. **40**, 279 (1978).
- [20] L. F. Abbott and P. Sikivie, Phys. Lett. B **120**, 133 (1983); J. Preskill, M. Wise and F. Wilczek, Phys. Lett. B **120**, 127 (1983); M. Dine and W. Fischler, Phys. Lett. **120**, 137 (1983); M. Turner, Phys. Rev. D **33**, 889 (1986); K. J. Bae, J. H. Huh and J. E. Kim, JCAP **0809** (2008) 005; L. Visinelli and P. Gondolo, Phys. Rev. D **80** (2009) 035024.
- [21] E. J. Chun and A. Lukas Phys. Lett. B **357**, 43 (1995);
- [22] J. E. Kim and M. -S. Seo, Nucl. Phys. B **864**, 296 (2012).
- [23] J. E. Kim and H. P. Nilles, Phys. Lett. B **138**, 150 (1984); E. J. Chun, J. E. Kim and H. P. Nilles, Nucl. Phys. B **370**, 105 (1992).
- [24] H. Murayama, H. Suzuki and T. Yanagida, Phys. Lett. B **291** (1992) 418.
- [25] K. J. Bae, H. Baer and H. Serce, Phys. Rev. D **91**, 015003 (2015) [arXiv:1410.7500 [hep-ph]].
- [26] P. Minkowski, Phys. Lett. B **67** (1977) 421; T. Yanagida, Conf. Proc. C **7902131** (1979) 95; M. Gell-Mann, P. Ramond and R. Slansky, Conf. Proc. C **790927** (1979) 315 [arXiv:1306.4669 [hep-th]]; R. N. Mohapatra and G. Senjanovic, Phys. Rev. Lett. **44** (1980) 912.
- [27] A. Kusenko and L. J. Rosenberg, arXiv:1310.8642 [hep-ph].
- [28] H. Baer, K. Y. Choi, J. E. Kim and L. Roszkowski, Phys. Rept. **555**, 1 (2014).
- [29] K. Y. Choi, J. E. Kim, H. M. Lee and O. Seto, Phys. Rev. D **77**, 123501 (2008).
- [30] H. Baer, A. Lessa, S. Rajagopalan and W. Sreethawong, JCAP **1106**, 031 (2011).
- [31] P. A. R. Ade *et al.* [Planck Collaboration], arXiv:1502.01589 [astro-ph.CO].
- [32] K. J. Bae, H. Baer, A. Lessa and H. Serce, JCAP **1410** (2014) 082.
- [33] L. Covi, H. -B. Kim, J. E. Kim and L. Roszkowski, JHEP **0105**, 033 (2001); A. Brandenburg and F. D. Steffen, JCAP **0408**, 008 (2004); A. Strumia, JHEP **1006**, 036 (2010).
- [34] E. J. Chun, Phys. Rev. D **84**, 043509 (2011)
- [35] K. J. Bae, K. Choi and S. H. Im, JHEP **1108**, 065 (2011)
- [36] K. J. Bae, E. J. Chun and S. H. Im, JCAP **1203**, 013 (2012).
- [37] K. A. Olive *et al.* [Particle Data Group Collaboration], Chin. Phys. C **38** (2014) 090001.
- [38] V. A. Kuzmin, V. A. Rubakov and M. E. Shaposhnikov, Phys. Lett. B **155** (1985) 36.
- [39] M. Carena, M. Quiros and C. E. M. Wagner, Nucl. Phys. B **524** (1998) 3; for an update, see M. Carena, G. Nardini, M. Quiros and C. E. M. Wagner, Nucl. Phys. B **812** (2009) 243.
- [40] K. J. Bae, H. Baer, V. Barger, D. Mickelson and M. Savoy, Phys. Rev. D **90** (2014) 7, 075010.
- [41] M. Fukugita and T. Yanagida, Phys. Lett. B **174** (1986) 45; M. A. Luty, Phys. Rev. D **45** (1992) 455; B. A. Campbell, S. Davidson and K. A. Olive, Phys. Lett. B **303** (1993) 63.
- [42] W. Buchmuller, P. Di Bari and M. Plumacher, Nucl. Phys. B **643** (2002) 367 [Nucl. Phys. B **793** (2008) 362]; W. Buchmuller, P. Di Bari and M. Plumacher, Phys. Lett. B **547** (2002) 128; P. Di Bari, AIP Conf. Proc. **655** (2003) 208 [hep-ph/0211175].

- [43] W. Buchmuller, R. D. Peccei and T. Yanagida, *Ann. Rev. Nucl. Part. Sci.* **55** (2005) 311; S. Davidson, E. Nardi and Y. Nir, *Phys. Rept.* **466** (2008) 105; S. Blanchet and P. Di Bari, *New J. Phys.* **14** (2012) 125012;
- [44] K. Kumekawa, T. Moroi and T. Yanagida, *Prog. Theor. Phys.* **92** (1994) 437; G. Lazarides, *Springer Tracts Mod. Phys.* **163** (2000) 227 [hep-ph/9904428]; G. F. Giudice, M. Peloso, A. Riotto and I. Tkachev, *JHEP* **9908** (1999) 014; T. Asaka, K. Hamaguchi, M. Kawasaki and T. Yanagida, *Phys. Lett. B* **464** (1999) 12; T. Asaka, K. Hamaguchi, M. Kawasaki and T. Yanagida, *Phys. Rev. D* **61** (2000) 083512; M. Kawasaki, M. Yamaguchi and T. Yanagida, *Phys. Rev. D* **63** (2001) 103514.
- [45] H. Murayama and T. Yanagida, *Phys. Lett. B* **322** (1994) 349.
- [46] M. Dine and A. Kusenko, *Rev. Mod. Phys.* **76** (2003) 1; K. Enqvist and A. Mazumdar, *Phys. Rept.* **380** (2003) 99; R. Allahverdi and A. Mazumdar, *New J. Phys.* **14** (2012) 125013.
- [47] K. Hamaguchi, H. Murayama and T. Yanagida, *Phys. Rev. D* **65** (2002) 043512.
- [48] I. Affleck and M. Dine, *Nucl. Phys. B* **249** (1985) 361.
- [49] M. Dine, L. Randall and S. D. Thomas, *Phys. Rev. Lett.* **75** (1995) 398; M. Dine, L. Randall and S. D. Thomas, *Nucl. Phys. B* **458** (1996) 291.
- [50] M. Y. Khlopov and A. D. Linde, *Phys. Lett. B* **138** (1984) 265; J. R. Ellis, D. V. Nanopoulos and S. Sarkar, *Nucl. Phys. B* **259** (1985) 175.
- [51] J. Pradler and F. Steffen, *Phys. Lett. B* **648**, 103 (1992).
- [52] R. H. Cyburt, J. R. Ellis, B. D. Fields and K. A. Olive, *Phys. Rev. D* **67** (2003) 103521; R. H. Cyburt, B. D. Fields, K. A. Olive and T. H. Yeh, arXiv:1505.01076 [astro-ph.CO].
- [53] M. Kawasaki, K. Kohri, T. Moroi and A. Yotsuyanagi, *Phys. Rev. D* **78** (2008) 065011.
- [54] K. Jedamzik, *Phys. Rev. D* **74**, 103509 (2006).
- [55] M. Flanz, E. A. Paschos and U. Sarkar, *Phys. Lett. B* **345** (1995) 248 [*Phys. Lett. B* **382** (1996) 447]; L. Covi, E. Roulet and F. Vissani, *Phys. Lett. B* **384** (1996) 169; W. Buchmuller and M. Plumacher, *Phys. Lett. B* **431** (1998) 354.
- [56] M. Plumacher, *Nucl. Phys. B* **530** (1998) 207.
- [57] S. Y. Khlebnikov and M. E. Shaposhnikov, *Nucl. Phys. B* **308** (1988) 885; J. A. Harvey and M. S. Turner, *Phys. Rev. D* **42** (1990) 3344.
- [58] W. Buchmuller, P. Di Bari and M. Plumacher, *Annals Phys.* **315** (2005) 305.
- [59] K. Hamaguchi, hep-ph/0212305.
- [60] H. Murayama and T. Yanagida, *Phys. Lett. B* **322** (1994) 349.
- [61] T. Gherghetta, C. F. Kolda and S. P. Martin, *Nucl. Phys. B* **468** (1996) 37.
- [62] K. Enqvist and J. McDonald, *Phys. Lett. B* **425** (1998) 309.
- [63] M. Fujii, K. Hamaguchi and T. Yanagida, *Phys. Lett. B* **538** (2002) 107.
- [64] R. Allahverdi, M. Drees and A. Mazumdar, *Phys. Rev. D* **65** (2002) 065010.
- [65] R. Allahverdi, B. A. Campbell and J. R. Ellis, *Nucl. Phys. B* **579** (2000) 355.
- [66] A. Anisimov and M. Dine, *Nucl. Phys. B* **619** (2001) 729.

- [67] M. Fujii, K. Hamaguchi and T. Yanagida, Phys. Rev. D **63** (2001) 123513.
- [68] H. Baer, A. Lessa and W. Sreethawong, JCAP **1201** (2012) 036.
- [69] K. J. Bae, H. Baer and A. Lessa, JCAP **1304**, 041 (2013).
- [70] K. Kohri, T. Moroi and A. Yotsuyanagi, Phys. Rev. D **73**, 123511 (2006).
- [71] H. Baer, S. Kraml, A. Lessa and S. Sekmen, JCAP **1104** (2011) 039.
- [72] K. J. Bae, H. Baer and E. J. Chun, JCAP **1312** (2013) 028.
- [73] F. E. Paige, S. D. Protopopescu, H. Baer and X. Tata, hep-ph/0312045;
<http://www.nhn.ou.edu/~isajet/>
- [74] H. Baer, C. Balazs and A. Belyaev, JHEP **0203**, 042 (2002).
- [75] K. J. Bae, H. Baer, V. Barger, M. R. Savoy and H. Serce, Symmetry **7** (2015) 2, 788.
- [76] K. J. Bae, H. Baer and E. J. Chun, Phys. Rev. D **89** (2014) 031701.